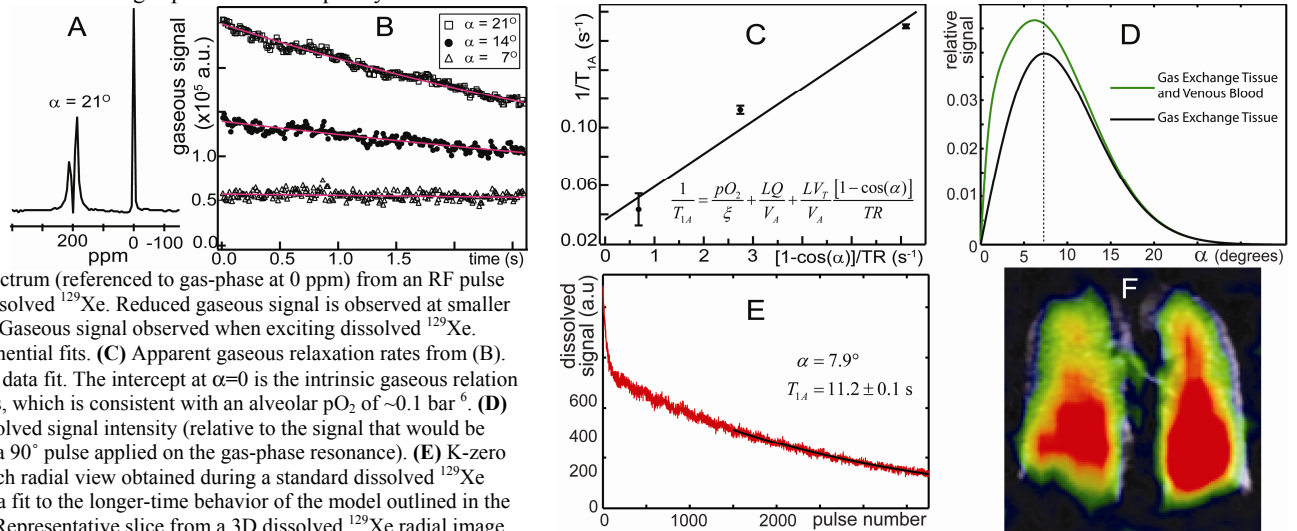


## Signal Dynamics during Dissolved-Phase Hyperpolarized $^{129}\text{Xe}$ Radial MR Imaging of Human Lungs

Z. I. Cleveland<sup>1,2</sup>, G. P. Cofer<sup>1,2</sup>, G. Metz<sup>3</sup>, D. Beaver<sup>3</sup>, J. Nouls<sup>1,2</sup>, S. Kaushik<sup>1,2</sup>, M. Kraft<sup>3</sup>, J. Wolber<sup>4</sup>, K. T. Kelly<sup>5</sup>, H. P. McAdams<sup>2</sup>, and B. Driehuys<sup>1,2</sup>  
<sup>1</sup>Center for In Vivo Microscopy, Duke University Medical Center, Durham, NC, United States, <sup>2</sup>Radiology, Duke University Medical Center, Durham, NC, United States, <sup>3</sup>Pulmonary and Critical Care Medicine, Duke University Medical Center, Durham, NC, United States, <sup>4</sup>GE Healthcare, Amersham, United Kingdom, <sup>5</sup>Radiation Oncology, Duke University Medical Center, Durham, NC, United States

**Introduction:** Direct MR imaging of HP  $^{129}\text{Xe}$  dissolved in the gas exchange tissues and capillary blood of rat lungs was recently demonstrated using a multiple breath, 2D radial imaging strategy.<sup>1</sup> In this work we extend these efforts to the direct, 3D imaging of dissolved HP  $^{129}\text{Xe}$  in humans. Because data acquisition in humans is confined to a single held breath, it is essential to make optimal use of the available dissolved  $^{129}\text{Xe}$  magnetization. Several Fick's 2<sup>nd</sup> Law-based models have been proposed to describe dissolved  $^{129}\text{Xe}$  dynamics within lungs<sup>1-4</sup> that yield information about alveolar surface-to-volume ratios<sup>4</sup>, dissolved Xe diffusion coefficients<sup>3</sup>, and interstitial barrier thickness<sup>1</sup>. However, these approaches, which rely upon infinite series solutions to the diffusion equation, are not well-suited to optimizing dissolved  $^{129}\text{Xe}$  MRI. Further, dissolved Xe excitations attenuate the source gas-phase magnetization through diffusive exchange<sup>3,5</sup> and, thus, indirectly reduce the dissolved  $^{129}\text{Xe}$  signal during imaging. In this work, we develop a more suitable mathematical framework for analyzing the dissolved HP  $^{129}\text{Xe}$  magnetization dynamics in the context of single-breath radial imaging in humans. Finally, because each radial view contains the k-zero value as the first data point, every image contains dynamic information that can be used to extract additional insights into global processes within the lungs using our model.

**Methods:** Studies were performed during a GE Healthcare sponsored, Phase I clinical trial for  $^{129}\text{Xe}$  MRI and involved 24 healthy volunteers who provided informed consent. Work was conducted under a GE Healthcare IND and approved by our IRB. MR data were obtained at 1.5 T using a GE EXCITE 14M5 MR scanner. Subjects received a 200 ml calibration and 4, 1-L doses of isotopically enriched Xe (83%  $^{129}\text{Xe}$ ) polarized to 6-9% using 2 prototype GE polarizers. Dissolved  $^{129}\text{Xe}$  images were acquired within a 16 s breath hold period using a constant flip angle, 3D radial sequence (3751 k-space views, matrix=32×32×32, FOV=40×40×48 cm<sup>3</sup>, TR/TE=4.2/0.9 ms, BW=15.6 kHz). Spectra were acquired with various BWs, TRs, and numbers of points. For both spectroscopy and imaging, dissolved,  $^{129}\text{Xe}$  was selectively excited using a 1.2 ms 3-lobe sinc pulse applied 3826 Hz above the gas phase  $^{129}\text{Xe}$  frequency.



**Fig. 1:** (A) Spectrum (referenced to gas-phase at 0 ppm) from an RF pulse centered on dissolved  $^{129}\text{Xe}$ . Reduced gaseous signal is observed at smaller flip angles (B) Gaseous signal observed when exciting dissolved  $^{129}\text{Xe}$ . Lines are exponential fits. (C) Apparent gaseous relaxation rates from (B). Line is a linear data fit. The intercept at  $\alpha=0$  is the intrinsic gaseous relaxation rate of  $T_{1,A} \sim 30$  s, which is consistent with an alveolar  $p\text{O}_2$  of  $\sim 0.1$  bar.<sup>6</sup> (D) Simulated dissolved signal intensity (relative to the signal that would be obtained from a  $90^\circ$  pulse applied on the gas-phase resonance). (E) K-zero values from each radial view obtained during a standard dissolved  $^{129}\text{Xe}$  image. Line is a fit to the longer-time behavior of the model outlined in the main text. (F) Representative slice from a 3D dissolved  $^{129}\text{Xe}$  radial image (color;  $\alpha=8^\circ$ ) overlaid on a gas-phase  $^{129}\text{Xe}$  SPGRE image (gray).

**Results:** Even when using a selective RF pulses, small levels of gaseous  $^{129}\text{Xe}$  are often excited (Fig. 1A). While this introduces a small level of off-resonant noise in imaging, the resulting spectra can be used to determine the contribution of dissolved  $^{129}\text{Xe}$  excitation to the apparent gas-phase relaxation rate ( $1/T_{1,A}$ ; Fig. 1 B,C). Using this information, three coupled 1<sup>st</sup> order differential equations can be constructed to describe the effects of relaxation, gas exchange, and pulmonary perfusion on the dissolved HP  $^{129}\text{Xe}$  magnetization. The solution to these equations, coupled with the effects of RF, is given below. A similar, but somewhat more complex, equation describes the magnetization present in the pulmonary venous blood.

$$M_T(n_-) = M_T(0) \left[ \cos^{(n-1)}(\alpha) e^{-(n-1)TR/T_{1T}} + \frac{\kappa}{(T_{1T}^{-1} - T_{1A}^{-1}(\alpha))} \left( \frac{e^{-TR/T_{1A}(\alpha)} - e^{-TR/T_{1T}}}{e^{-TR/T_{1A}(\alpha)} - \cos(\alpha)e^{-TR/T_{1T}}} \right) \left( e^{-(n-1)TR/T_{1A}(\alpha)} - \cos^{(n-1)}(\alpha) e^{-(n-1)TR/T_{1T}} \right) \right]$$

In the equation,  $1/T_{1T}$  is the apparent relaxation rate in tissues, which depends upon diffusion, relaxation, and perfusion.  $\kappa$ , which is on the order of  $100 \text{ ms}^{-1}$ , is the rate of diffusive magnetization replenishment in the gas exchange tissues, and  $M_T(n_-)$  is the dissolved magnetization present immediately before the  $n^{\text{th}}$  RF pulse. This model indicates that the initial dissolved magnetization dynamics are dominated by the interplay of RF attenuation and diffusive replenishment of dissolved magnetization. The longer-time dynamics are dominated by the apparent gas-phase relaxation rate of HP  $^{129}\text{Xe}$ , which depends indirectly on the RF attenuation. Further, it is possible to define an 'optimum' flip angle that minimizes image distortions due to signal decay throughout the image acquisition by maximizing the signal intensity obtained from the final RF pulse. A simulation demonstrating the flip angle dependence of the final signal intensity, based on our model, is shown in Fig. 1D. These results suggest that dissolved  $^{129}\text{Xe}$  MRI is optimized by using rather large flip angle RF pulses ( $>6^\circ$ ), which is in agreement with our empirical observations (Fig. 1F).

**Conclusions:** Directly imaging HP  $^{129}\text{Xe}$  dissolved in human lungs within a single, 16 s breath hold is feasible using 3D radial imaging. The image quality obtained from dissolved  $^{129}\text{Xe}$  is optimized by using relatively high ( $\sim 8^\circ$ ) RF pulses. This observation can be rationalized in light of a relatively simple, closed-form mathematical model, which incorporates known pulmonary physiology including perfusion,  $\text{O}_2$  partial pressure, and gas exchange tissue volume. These results also highlight a unique advantage of radial imaging, which allows information about whole-lung magnetization dynamics to be extracted from raw image data.

**Acknowledgements:** GE Healthcare, HL 5R21HL87094, Philip Morris External Research Fund, Center for In Vivo Microscopy P41 RR005959

**References:** (1) B Driehuys, et al. *PNAS* **2006**, 103, 18278-18283. (2) S Mansson, et al. *MRM* **2003**, 50, 1170-1179. (3) K Ruppert, et al. *MRM* **2004**, 51, 676-687. (4) S Patz, et al. *Proc. 16<sup>th</sup> ISMRM* **2008**. (5) K Ruppert, et al. *MRM* **2000**, 44, 349-357. (6) CJ Jameson, et al. *J Chem Phys* **1988**, 89, 4074-4081.